β decay of ^{66}Co, ^{68}Co, and ^{70}Co

W. F. Mueller,* B. Bruyneel, S. Franchoo,† M. Huyse, J. Kurpeta, K. Kruglov, Y. Kudryavtsev, N. V. S. V. Prasad,
R. Raabe, I. Reusen, P. Van Duppen, J. Van Roosbroeck, L. Vermeeren, and L. Weissman†
Instituut voor Kern- en Stralingsfysica, University of Leuven, B-3001 Leuven, Belgium

Z. Janas, M. Karny, T. Kszczot, and A. Płochocki
Insitute of Experimental Physics, Hoza 69, 00-681 Warsaw, Poland

K.-L. Kratz and B. Pfeiffer
Institut für Kernchemie, Universität Mainz, D-55099 Mainz, Germany

H. Grawe
Gesellschaft für Schwerionenforschung, D-64291, Darmstadt, Germany

U. Köster
Physik-Department, Technische Universität München, D-85748 Garching, Germany

P. Thirolf
Sektion Physik, Universität München, D-85748 Garching, Germany

W. B. Walters
Department of Chemistry, University of Maryland, College Park, Maryland 20742

The neutron-rich nuclei, ^{66}Co, ^{68}Co, and ^{70}Co were produced using a laser-ionization isotope-separation on-line method. The resulting β-delayed γ decay was studied. The half-life of ^{66}Co is measured to be 0.18(1) s. Two β-decaying states are identified in ^{68}Co with half-lives of 0.23(3) and 1.6(3) s. In addition, two β-decaying states are observed in ^{70}Co with half-lives of 0.12(3) and 0.50(18) s. From the β decay of these states in ^{66,68,70}Co, many new excited levels are established in ^{66}Ni, ^{68}Ni, and ^{70}Ni. These results are compared to the valence mirror nuclei in the $N=50$ region as well as with shell-model calculations. It can be concluded that collective excitations appear to play an increasingly important role with increasing occupation of the $\nu g_{9/2}$ orbital.

PACS number(s): 21.10.−k, 23.20.−g, 23.40.Hc, 27.50.+e

I. INTRODUCTION

The structure of nuclei in the region around neutron-rich nuclei with $Z\sim28$ has been a subject of considerable study by numerous groups. Early studies by Bernas *et al.* [1,2] resulted in the first identification and β-decay half-life measurements of ^{68}Co and ^{69}Co nuclei. Direct mass measurements for $^{66-69}$Co and $^{67-72}$Ni later fixed the Q_β values for a large number of nuclei [3]. The first observation of ^{78}Ni was reported by Engelmann *et al.* [4]. In-beam studies of $^{64-67}$Ni produced by deep-inelastic collisions were performed by Pawłat *et al.* [5], and ^{68}Ni was studied with similar methods by Broda *et al.* [6]. The half-lives of $^{70-72}$Co and $^{73-76}$Ni were reported by Ameil *et al.* [7]. Half-lives of nuclei from ^{57}Ti to ^{70}Co have been presented recently in Ref. [8]. Despite the number of studies, the identification of excited states in these nuclei has been rare. This is primarily

due to the difficulty of producing clean sources in sufficient intensity for spectroscopic studies. Excited states in ^{69}Ni and ^{70}Ni were recently identified from the decay of μs isomers [9], and β-delayed γ decay of Ni nuclei up to mass 74 has been reported in Ref. [10]. In order to further study the structure of Ni isotopes, a program to measure the β-delayed γ decay of $^{66-70}$Co was started. The results of the ^{67}Co and ^{69}Co decay are presented in Refs. [11,12]. In this paper the β-decay results for ^{66}Co, ^{68}Co, and ^{70}Co are described and discussed.

The motivation for these experiments comes from the desire to study neutron-rich nuclei below the $N=50$ major shell gap with the eventual goal of studying the structure of the doubly magic ^{78}Ni. ^{78}Ni is the most neutron-rich double-magic nucleus that can be reached in the near future. While there are many predictions for this nucleus, it is not definitely known what effect such a large neutron excess would have on the structure of ^{78}Ni. In addition, the details of the structure of nuclei in this region and ^{78}Ni in particular are important input for the astrophysical r-process model [13].

For nuclei with $40<N\leq50$ the $\nu g_{9/2}$ orbital is the most important one for determining their structure. Critical to understanding the influence of the $\nu g_{9/2}$ orbital on the structure

of nuclei in this region is knowing what structure changes occur just as the $g_{9/2}$ orbital becomes occupied (i.e., $38 \leq N \leq 42$). To this end, β-delayed γ rays resulting from the decay of ^{66}Co, ^{68}Co, and ^{70}Co have been measured. The daughters of these nuclei are Ni isotopes which, with $Z = 28$, have a closed proton shell. For the neutrons, the gap at $N = 40$ between the $g_{9/2}$ orbital and the fp shell ($p_{3/2}$, $f_{5/2}$, and $p_{1/2}$) was shown to have an increased stabilizing effect on the structure of ^{68}Ni$_{40}$ [1,6], however, this effect was shown to be very tenuous in that most of the semi-double-magic properties observed in ^{68}Ni disappear with the addition of a single nucleon [12]. ^{66}Ni$_{38}$ is a representative case where the occupation of the $g_{9/2}$ orbital is small, and thus the $g_{9/2}$ influence is less significant, while ^{70}Co$_{42}$ is fully within the $g_{9/2}$ shell. By using the selective nature of β decay, it is possible to study the changes in structure of these three nuclei as the $g_{9/2}$ orbital becomes increasingly occupied.

II. EXPERIMENTAL SETUP AND ISOTOPE YIELDS

Neutron-rich Co nuclei were produced in a 30-MeV-proton-induced fission reaction of ^{238}U at the Louvain-la-Neuve cyclotron facility. The two ^{238}U target foils, with thicknesses of 15 mg/cm^2 each, were arranged within the gas cell of the Leuven ion-guide laser-ion source (LIGLIS). The fission products recoil out of the targets and into the cell which contains purified Ar gas at a pressure of 500 mbar. The recoils become neutralized in the gas and are transported by the gas flow to the exit hole of the cell. Near the exit hole, the Co isotopes are selectively ionized with two EXIMER-pumped dye lasers set at pulse-repetition rates of 200 Hz and tuned to resonant excitations of Co with 230.903 and 481.90 nm, respectively. The charged isotopes are extracted from the gas cell and guided to the entrance of the LISOL mass separator with a sextupole ion guide. The products are then selected by their A/q ratio and transported to the detection point. The details of the LIGLIS-LISOL setup can be found in Refs. [14–16].

While the beam is on target the high plasma density caused by the reaction in the gas cell make laser ionization significantly less efficient, and as a result measurements during "beam-on" periods are not practical. Thus the proton beam was pulsed with a "microcycle" of 100 ms on and off, respectively. During the "beam-on" cycle, isotope transmission through the mass separator is suppressed. In order to measure the half-life of the Co nuclei, the cyclotron and mass separator was also set in a "macrocycle" where the pulsed beam was on target for 0.6 s followed by a 1.0 s beam off period. A second "macrocycle" of 2.4/4.0 s beam on/off was also used to study the isomeric decay of ^{68}Co. Spectra were taken with the laser on resonance with the Co atomic transitions as well as with the lasers turned off. The lasers off spectra can be used to identify the nonresonant γ lines in the specific mass chain. The ratio between the intensity of the Co lines in the lasers on spectra relative to the lasers off defines the selectivity of the laser ion source. This ratio is typically 30.

The setup at the detection point consisted of two high-purity Germanium detectors (70% and 75% relative effi-

ciency) and three ΔE plastic detectors arranged in a compact configuration. The trigger for the data acquisition system was set to accept β-γ and γ-γ coincidence events. In addition, multiscaled Ge singles were collected by a separate system. Long-lived daughter products as well as other background contamination at the detection point were removed by periodically moving the implantation tape. Further details about the detector setup can be found in Ref. [17]. Earlier experiments to measure $^{68-74}$Ni were also performed with the LIGLIS-LISOL setup with similar detector configurations. The results from the measurements of Ni are presented in Refs. [10,12]. Details of the isotope yields from these experiments are presented here with the results from measurements of $^{66-70}$Co.

The isotope yields of Ni and Co nuclei obtained from the laser ion source are shown in Table I and illustrated in Fig. 1. When possible the yields are determined from the strongest clean γ ray resulting from the β decay of the nucleus of interest. For the case of several of the Ni isotope (noted in the table) decays, the γ-ray branching ratios could not be accurately determined; however, the purity of the ion source was such that the yield of these nuclei could be determined from γ rays resulting from the decay of the daughter. Very recently, improvements were made to the laser ion source that resulted in an $\approx 450\%$ increase in the yield from the source. These recent developments will be presented in a future publication [18]. The new yields for ^{66,67}Co and ^{71}Ni are presented in the lower part of Table I and as open symbols in Fig. 1. For the discussions of systematic trends of the yields, the older values will be used.

Shown with the experimental yields in Fig. 1 are the results of theoretical calculations of the fission-product cross sections by Rubchenia and first presented in Ref. [19]. Here the question arises, whether the experimental yields are, as the theoretical ones, independent yields and not cumulative ones. Due to the decreasing isotopic yield in this very asymmetric fission with decreasing Z number this effect could only be present for some specific cases. According to the calculations only in the mass chains with $A < 69$, the Co nuclei produced more than the Ni nuclei. But as can be calculated from the comparison of the spectra taken with and without lasers, the strong Z selectivity of the laser ionization rules out the effect of nonresonantly ionized isobars. Another possible cumulative effect is decay in the gas cell. Indeed the delay time in the gas cell is of the order of ~ 100 ms. By inspecting the different isobars (see Table I) only the summed yield of ^{68}Co (1.6 at/μC) comes in the neighborhood of ^{68}Ni (3.6 at/μC). The half-lives of the ^{68}Co isomers are 1.6 and 0.23 s (see further) which means that only the short-living isotope could substantially decay during transport. The 100 ms on/100 ms off production cycle, the inhomogeneous stopping pattern of the fission products in the gas cell and the complicated evacuation pattern makes it difficult to exactly calculate the correction needed for the independent yield of ^{68}Ni but considering the relative production (0.9 versus 3.6 at/μC) and the relative time scale (230 versus 100 ms), we estimate that the effect is less than 10% and thus well within the error bars.

The scale for the theoretical values in Fig. 1 is chosen

TABLE I. Experimentally determined yields of $^{68-74}$Ni and $^{66-70}$Co isotopes out of the Leuven laser ion source. The three yield values below the separation are from more recent experiments.

Nucleus	Measured time (h)	γ-ray energy (keV)	γ-ray branch	Yield (at/μC)
^{68}Ni	25.05	1078[a]	64%	3.6(7)
^{69}Ni (h.s.)	9.02	205	27%	4.3(8)
^{69}Ni (l.s.)	9.02	1298	74%	0.7(3)
^{70}Ni	5.40	885[a]	93%	6(1)
^{71}Ni	35.16	534	59%	3.0(6)
^{72}Ni	11.86	653[a]	68%	1.1(2)
^{73}Ni	28.65	450[a]	45%	0.26(6)
^{74}Ni	13.19	606[a]	79%	0.034(9)
^{66}Co	0.75	1425	100%	0.4(2)
^{67}Co	3.03	694	95%	2.6(8)
^{68}Co (h.s.)	40.38	272	44%	0.9(4)
^{68}Co (l.s.)	40.38	2033	95%	0.7(3)
^{69}Co	9.56	594	54%	0.8(3)
^{70}Co (h.s.)	26.33	970	100%	0.052(15)
^{70}Co (l.s.)	26.33	608	27%	0.10(3)
^{71}Ni	0.08	534	59%	12(5)
^{66}Co	5.00	1425	100%	1.8(7)
^{67}Co	0.08	694	95%	12(5)

[a]Cu daughter line.

such that the maximum cross section for a given isotope chain is approximately equivalent to the maximum experimental yield for that chain. From this comparison one can see that the slope of the fission yields are resonably well reproduced; however, the point of maximum cross section for both Ni and Co is approximately one mass unit farther from stability than what was observed in the experimental yields.

It should be noted that a more accurate comparison of the experimental yields to the theoretical cross sections requires
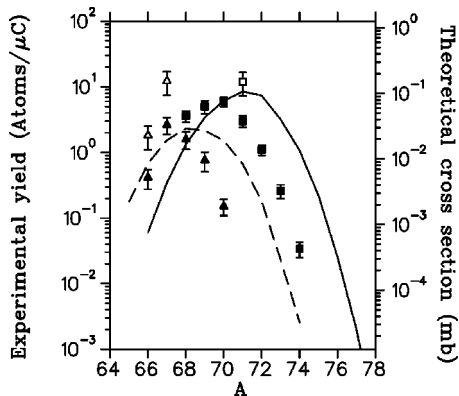

FIG. 1. Experimental yields extracted from the LIGLIS. The filled and open squares (triangles) correspond to early and improved yields for Ni (Co), respectively. The values are plotted according to the scale on the left-hand vertical axis. The solid (dashed) line corresponds to the calculated fission cross sections of Ni (Co) isotopes, plotted with respect to the right-hand vertical axis. For nuclei with isomers, the sum of the two yields is plotted.

that corrections be made for possible losses due to the delay time for extraction from the gas cell. This delay depends on where the fission products are stopped in the gas cell. While this delay time is estimated to be ≈ 100 ms from the middle of the cell, the delay from certain locations in the cell could be as long a second. This effect is likely negligible for Ni, but for the short-living Co isotopes, a correction should be made for each isotope. As the modeling of the gas transport and atom-ion survival probability is quite complicated, reliable corrections are not yet possible. However, the effect for the Ni isotopes is neglible as the half-lives of the involved isotopes are in the seconds range. In contrast, the Co nuclei under study have half-lives ranging from 120 ms to 1.6 s. Strangely the shortest living isotopes in the Co yield curve are at the extremes: ^{66}Co has a half-life of 180 ms and ^{70}Co(high spin) has a 120 ms half-life (see Table II). The other isotopes are longer-living and thus a correction for decay loss will mainly increase the extremes of the Co curve but the point of maximum cross section will hardly be affected. However, decay losses could partially explain why the ^{66}Co yield differs so dramatically from the systematic trend.

III. RESULTS

A. ^{66}Co

The β-delayed γ decay data for ^{66}Co were collected over a period of 5 h with the improved LIGLIS setup. A representative β-gated γ-ray spectrum from this measurement is shown in Fig. 2. In this spectrum two strong lines of 1246.1(2) and 1425.9(2) keV were observed with relative

TABLE II. Proposed spins and parities (I^π), and measured half-lives for β-decaying states in ^{66}Co, ^{68}Co, and ^{70}Co nuclei. Also presented are the results from previous measurements and calculations ($t_{1/2}^{th}$) using two different models. The theoretical results and their meanings are discussed in Sec. V.

	I^π	$t_{1/2}$ (s) this work	$t_{1/2}$ (s) literature	$t_{1/2}^{th}$ (s) Nil-BCS	$t_{1/2}^{th}$ (s) FY-LN
^{66}Co	(3^+)	0.18(1)	0.23(2) [20], 0.24(3) [21]	0.137	0.212
^{68}Co (high spin)	(7^-)	0.23(3)	0.18(10) [2], 0.17(3) [8]	0.0927	0.138
^{68}Co (low spin)	(3^+)	1.6(3)	First observation	0.533	0.508
^{70}Co (high spin)	$(6^-,7^-)$	0.12(3)	0.15(2) [7], 0.092(25) [8]	0.0420	0.0653
^{70}Co (low spin)	(3^+)	0.50(18)	First observation	0.451	0.319

intensities of 69(5) and 100(4), respectively. These lines were initially reported in a previous β-decay study [20], and later confirmed from in-beam work [5]; however, a 471-keV γ ray reported in Ref. [20] was not observed despite having sufficient statistics to measure it. Thus it is likely that this γ ray was incorrectly assigned. There is, however, an additional line identified at 1804.7(2) keV with a half-life consistent with the decay of ^{66}Co. The intensity of this transition relative to the 1426-keV line ($\equiv 100$) is 9(2). Additional lines observed in Fig. 2 are attributed to contamination from ^{112}Ag present from ^{112}Rh$\rightarrow^{112}$Pd$\rightarrow^{112}$Ag decay which was implanted next to the tape in the detection system during optimization of the laser-ion source. The half-life of ^{66}Co is determined from a sum of spectra gated on the 1246 and 1426-keV time-decay γ rays (Fig. 3). The resulting half-life from a fit of these data is 0.18(1) s and is listed in Table II. This value is slightly smaller but in general agreement with the previously measured values of 0.23(2) s [20] and 0.24(3) s [21].

Analysis of the γ-γ coincidence data revealed that the 1426 and 1246-keV γ rays are in coincidence; however, the statistics were not sufficient to confirm whether the 1805-keV transition is coincident with either of these two lines. Placement of this 1805-keV γ ray feeding the ground state would be inconsistent with what is observed from (t,p) [22] and $(\alpha,2p)$ [23] transfer reactions; however, a 2^+ excited state reported at 3219(10) keV in Ref. [22] is consistent with the 1804-keV γ ray feeding the 1426-keV level. The resulting decay scheme based on these observations is presented in Fig. 4. The β branching ratios are determined from the relative γ-ray intensities and the log ft values are deduced using the Q_β energy from Ref. [20], and the log f tables of Gove and Martin [24].

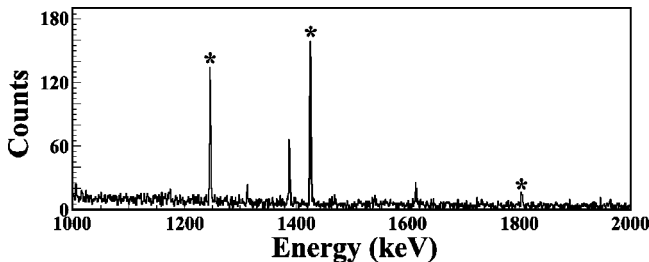FIG. 2. Representative β-gated γ-ray spectrum for $A=66$ when lasers are tuned to Co resonance. The asterisks indicate lines identified with the decay of ^{66}Co.

One of the differences in the decay scheme presented here compared to previous work is that the β feeding to the 2_2^+ state at 2900 keV could not be confirmed; however, rather strong feeding to the 2_3^+ state at 3231 keV is observed with a log ft value of 4.5. In addition, there is direct β feeding to the 2_1^+ with a log ft of 5.0, but it should be noted that feeding from unresolved γ rays can contribute false β intensity to this level.

B. ^{68}Co

Excited states in ^{68}Co were positively identified by comparing the β-delayed γ spectra with laser irradiation to corresponding spectra without lasers. Representative Ge energy spectra illustrating this comparison are shown for $A=68$ in Fig. 5(a) for lasers tuned to Co resonance and in Fig. 5(b) for lasers turned off. The number of events in the lasers-off spectrum has been renormalized to reflect the same measuring time used to produce Fig. 5(a). As can be seen in these figures, there are a significant number of lines (indicated with asterisks) that are present in Fig. 5(a) and completely missing in Fig. 5(b). These are the transitions that can be positively associated with the decay of ^{68}Co. The strongest lines present in the lasers-off spectrum are largely the result of $(^{96}$SrAr$)^{+2}$ molecules and ^{68}Ni^{+1} nuclei that are not fully neutralized in the gas cell.

A listing of the γ rays and their relative intensities observed to be Co resonant at $A=68$ is presented in Table III. The time decay analysis of these γ rays reveals two distinct half-lives which clearly indicates that there are two β-decaying states in ^{68}Co. These two half-lives can been seen in Fig. 6 where panel (a) is the decay curve resulting from a background subtracted sum of gates of the γ rays in right-hand columns of Table III, and panel (b) a sum of gates of the γ lines in the left columns. The spectrum in the inset of Fig. 6(b) was produced from the 0.6/1.0-s macrocycle data, while the main body figures are from the 2.4/4.0-s macrocycle. Representative fits to the data are also presented in Fig. 6, and the results of these measurements are 1.6(3) s and 0.23(3) s for the long and short half-life, respectively. These results are also presented in Table II. A half-life of 0.18(10) s was previously measured by Bernas *et al.* [2] and recently reported as 0.17(3) s by Sorlin *et al.* [8]. These two results are consistent with the short half-life that is observed here. It is interesting to note that the long half-life state was not observed in either experiment.

In consideration of the two half-lives, the β-gated spectra, as well as γ-γ coincidence data, a decay scheme for ^{68}Co can be determined. This scheme is presented in Fig. 7. Previous to this work, excited states in ^{68}Ni were observed in two-proton transfer reactions [1,25] and deep-inelastic collisions [6]. In the experiment of Bernas *et al.* [1], the first excited 0^+ state was observed at an energy of 1.77(3) MeV with a measured half-life of 211(50) ns. Later Girod *et al.* [25] reported on a direct observation of excited states in ^{68}Ni; however, the typical uncertainties on the level energies were greater than 30 keV. Broda *et al.* [6] positively established the first 2^+ and 5^- states at energies of 2.033 and 2.847 MeV, respectively. In addition, they observed that the 5^- level is isomeric with a half-life of 0.86(5) ms. Very recently, Ishii *et al.* [26] observed an 8^+ 23(1) ns isomer at 4208 keV. Presented in this article is the first study of β-delayed γ rays from ^{68}Co.

From the analysis of the γ rays characterized by the short half-life, the 114, 324, and 273-keV γ rays are observed in cascade, and from coincidence and sum energy considerations the 595 and 709-keV γ rays are placed as crossover transitions. No other coincidences are observed with these γ rays; in particular, no coincidence is observed with the 2033-keV transition. As a consequence, the likely placement of these short-half-life γ rays would be feeding the 5^- isomer. Support for this assignment comes from the fact that the observed half-life of the 815-keV γ ray feeding out of the 5^- isomer is also 0.23 seconds. It is interesting to note, that Ishii *et al.* [26] have also observed this γ-decay structure being fed from the 8^+ isomer. In addition, they observe a 377-keV γ ray feeding into these levels. This γ ray is only very weakly observed in the β decay and is placed in the decay scheme based on their data.

Of the γ rays with a long half-life, seven are observed to be coincident with the 2033-keV transition, while the 2745, 1139, 694, and 511-keV γ lines are not. The 1115, 3483, 3520, and 3745-keV γ rays are placed directly feeding the 2033-keV level. A 663-keV line is also observed to be weakly coincident with the 2033-keV transition, however, its intensity is too weak to make a conclusive assignment. Thus this γ ray is currently left unplaced. From the observation of coincidence relationships of the 1422-keV γ ray, the 2745-keV line can be positively established as a transition bypassing the 2033 and 1770-keV levels.

A rather surprising result from the measurements is the observation of a level at 2511 keV, which is established by an observed coincidence between the 2033 and 478-keV γ rays. These two γ rays are also in coincidence with the 1515-keV transition. Inverting the 1515 and 478 transitions (i.e., having the 1515-keV transition directly feed the 2033-keV level) was considered, but the 478-keV γ ray is ~50% more intense than the 1515-keV transition and there are no unplaced γ rays with sufficient intensity to explain this imbalance. In addition, the number of 478-2033 coincidences is consistent with the entire intensity of the 478-keV γ ray feeding the 2033-keV level. Results from transfer reactions [25], unfortunately cannot confirm the existence of this level, because the region corresponding to excitation energies be-

tween 2.2 and 2.7 MeV was strongly contaminated, thus, making level assignments in this region impossible.

The 694 and 1139-keV γ-rays have long half-lives but neither is observed to be coincident with any other γ lines. It can be ruled out that these γ rays feed the 0_2^+ level, because coincidence with the 511-keV γ rays that would result from the $0_2^+ \rightarrow 0_1^+$ internal pair creation is not observed. In both cases, placement of these two γ rays feeding the ground state is inconsistent with previous observations, thus they most likely directly feed the 5^- isomer at 2848 keV. The intensity of these lines is sufficiently weak compared to the short half-life γ rays that their long half-lives would not significantly influence the half-life of the 815-keV line.

Also observed in the Co-resonant β-gated γ ray spectrum is a significant excess of 511-keV γ rays. Nearly all the 511 intensity can be accounted as 511-511 coincidences as well as being coincident with β particles. In addition, this γ line has a measured half-life consistent with the decay from the state with the 1.6 s half-life. The fact that this 511-keV intensity is self-coincident implies that it is not caused by pair production from high-energy γ rays interacting inside the germanium detectors; rather, it is likely that the 511 intensity is the result of internal pair creation at the source caused by an $E0$ transition. Note that these 511-keV lines appear prompt with β particles to within the ≈ 15 ns time resolution of the experimental setup; thus, it can be ruled out that the 511 originates from the decay of the 0_2^+ level which has an observed half-life of 211(50) ns [1]. A source of this 511 intensity may be from decay of the 2511-keV excited state to the ground state. This possibility will be discussed in more detail in Sec. IV B.

The β feeding of the levels in Fig. 7 are determined from the comparison of the relative γ-ray intensities measured in β-gated Ge spectra [e.g., Fig. 5(a)]. It should be noted that the lower excited states (e.g., the 2033, 2511, and 2745-keV levels) also have significant intensity imbalance which could be interpreted as β feeding; however, the imbalance for these levels can also be the result of unresolved γ decay from higher levels. The amount of unresolved γ feeding can be determined from the total number of γ-ray events in a β-γ-γ spectrum gated on the 2033-keV γ ray. The total amount of observed relative β-gated γ-ray intensity coincident with the 2033-keV transition is determined from Table III to be 58(4). By considering the total γ-ray interaction efficiency for the two germanium detectors in the setup ($\approx 29\%$) and normalizing on the total number of 2033-keV events in the
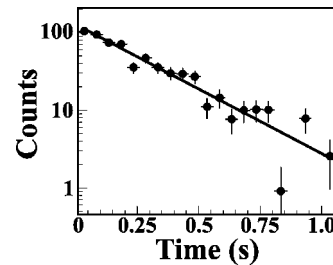

FIG. 3. Time dependent spectrum with representative decay fit resulting from the sum of gates on 1426- and 1246-keV γ rays.
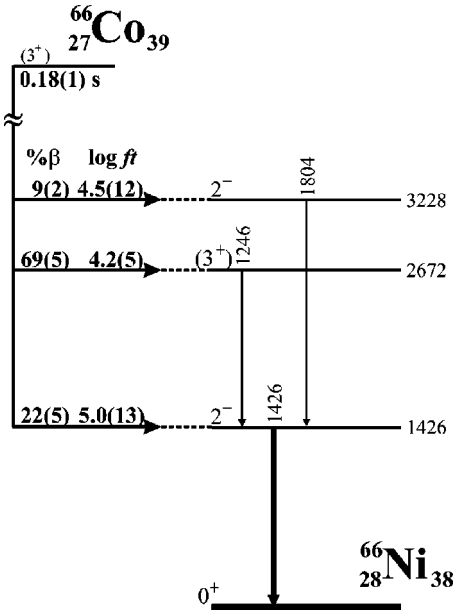
$^{66}_{27}\text{Co}_{39}$

(3^+)

0.18(1) s

%β   log *ft*

9(2) 4.5(12) 2^- 3228

1804

69(5) 4.2(5) (3^+) 2672

1246

22(5) 5.0(13) 2^- 1426

1426

$^{66}_{28}\text{Ni}_{38}$

0^+

FIG. 4. The decay scheme for ^{66}Co.

β-γ spectrum, one expects a total of 165(11) events in the 2033-gated β-γ-γ spectrum. Experimentally one observes 176(19) events in this spectrum; thus one can conclude that within the uncertainty of the comparison there is no direct β feeding to the 2033-keV level. From similar procedures, one can also conclude that there is very little feeding to the 2511 and 2745-keV levels; however, the uncertainty in these deductions is significantly greater than for the 2033-keV state. While it is not statistically significant to make the same analysis for higher energy states, γ-ray feeding to these levels becomes decreasingly likely with increasing excitation energy. Thus ≈50% of the β decay of the low-spin state in ^{68}Co likely proceeds via unresolved levels that subsequently γ decay to the 2033, 2511, and 2745-keV levels. Consequently, the β-decay feeding to the 2033, 2511, and 2745-keV levels are shown as limits to reflect the fact that the β branching ratios are likely not from direct feeding.

C. ^{70}Co

Similar to ^{68}Co, γ rays can be unambiguously associated with the decay of ^{70}Co by comparison of $A = 70$ spectra
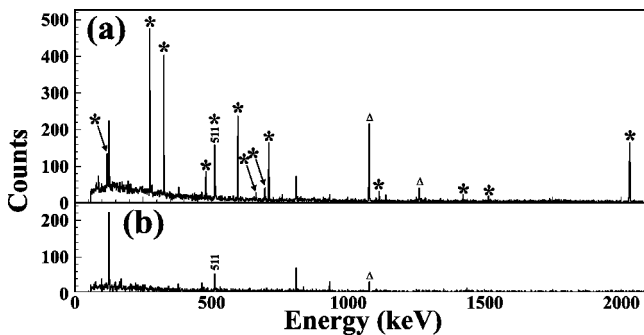

FIG. 5. Representative β-gated γ-ray spectra for $A = 68$ when (a) lasers are tuned to Co resonance and (b) lasers are off. The asterisks indicate lines that can be positively associated with ^{68}Co decay and triangles indicate γ rays from the ^{68}Ni daughter decay.

TABLE III. Energy, relative intensity, and half-life identification of γ rays measured in β-gated decay spectra of ^{68}Co. The left columns correspond to the γ rays with 0.23(3) s half-lives, and the right columns those with 1.6(3) s half-lives. The intensities are normalized with respect to the isomer from which they originate.

$t_{1/2} = 0.23(3)$ s		$t_{1/2} = 1.6(3)$ s	
Energy (kev)	Intensity (relative)	Energy (keV)	Intensity (relative)
113.5(2)	20.2(5)	477.8(2)	15.5(7)
271.9(2)	≡100(2)	511.2(2) [b]	20.8(5)
323.6(2)	88.4(17)	663.2(5)	3.4(2)
377.4(5)[a]	3.4(3)	694.3(2)	7.6(3)
595.2(2)	74.1(17)	708.9(2) [c]	6.0(4)
708.9(2)[c]	46.9(12)	1115.1(2)	9.7(5)
815.0(2)	230(22) [d]	1139.4(2)	6.2(4)
2033.2(2)	230(22) [d]	1422.0(2)	10.6(6)
		1514.8(2)	10.2(5)
		2033.2(2)	≡100(2)
		2744.6(2)	14.7(8)
		3479(2)	7.4(7)
		3516(2)	5.5(7)
		3741(2)	10.3(7)

[a]The statistics for this level were insufficient to conclusively determine the half-life of the 377-keV γ ray. half-life assignment is made on the basis of the observed decay, as discussed in the text.
[b]The intensity of the 511-keV line originates from electron-positron annihiliation and is accounted as such in the determination of its intensity.
[c]Based on coincidence conditions and half-life measurements, the 708.9-keV γ ray is a doublet.
[d]The intensity of the 815-keV and 2033-keV γ rays are determined from γ-γ coincidence.

when lasers are tuned to Co and lasers are turned off, respectively. Spectra illustrating this comparison are presented in Fig. 8. The contamination from non-neutralized fission products with the same Q/A ratio is significantly greater for mass 70 compared to mass 68. Nevertheless, the ^{70}Co γ ray lines (indicated by asterisks in Fig. 8) are clearly gone in the lasers off spectrum [Fig. 8(b)] thus establishing their identity. The γ rays identified by this method are presented in Table IV.

Excited states in ^{70}Ni have been initially observed in μs isomer studies by Grzywacz *et al.* [9]. From that study, a cascade of four γ rays was identified as resulting from the decay of an 8^+ seniority isomer. The same γ rays up to the 6^+ level are observed in β-gated spectra. In addition a new γ ray of 682 keV is observed in coincidence with these transitions. These γ lines have a measured half-life of 0.12(3) s. The previously reported 0.15(2) s [7] and 0.092(25) s [8] measurements are consistent with this observation. Time-decay spectra illustrating this decay is presented in Fig. 9(a). Another new level at 1868 keV is established by an observed coincidence between the 1259-keV $2^+ \rightarrow 0^+$ transition and a 608-keV transition, as well as the existence of a 1868-keV crossover γ ray. As can be seen in Fig. 9(b), the time-decay spectrum of the sum of the 608 and 1868-keV transitions shows a half-life of 0.50(18) s. Thus, similar to ^{68}Co, there
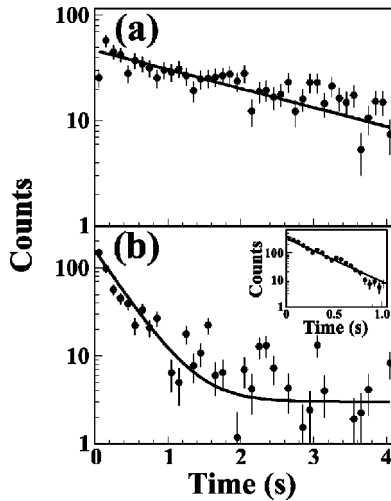
FIG. 6. Time-dependent spectra for the 2.4/4.0 s macrocycle when (a) gated on long half-life γ rays of Table III and (b) short half-life γ rays. The inset of panel (b) shows the time-dependent spectrum for the 0.6/1.0 s macrocycle when gated on short half-life γ rays. The thick lines show the results of decay fits to the data.

are two β-decaying states in ^{70}Co. These half-lives are presented in Table II with the ^{66}Co and ^{68}Co values. An additional γ ray at 1256 keV is clearly Co resonant and has a half-life consistent with the longer-lived isomer decay of ^{70}Co, but it is not observed to be coincident with other γ rays; however, the intensity is sufficiently weak that coincidences with other transitions in ^{70}Ni cannot be ruled out.
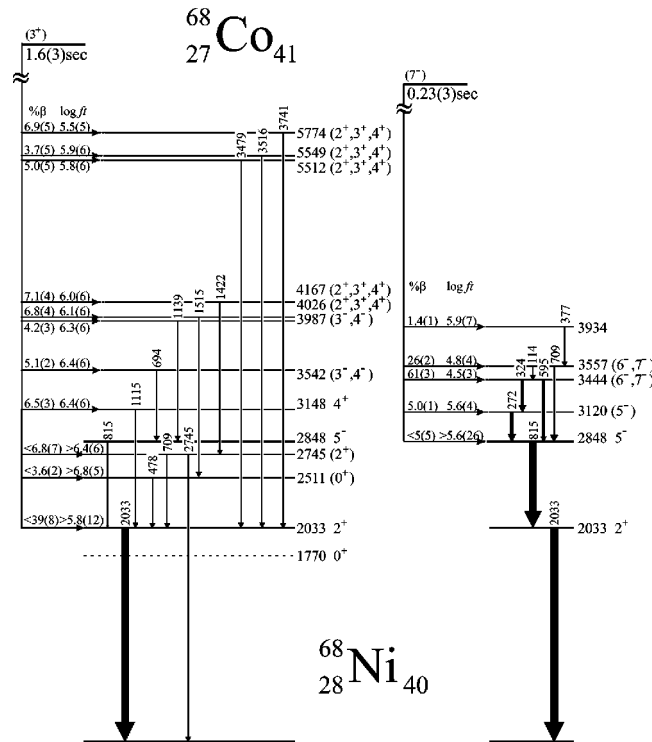

FIG. 7. The decay schemes for ^{68}Co. Decay of the two isomers are shown separately with proposed spins and parities for levels given to the right of the excitation energy of the respective schemes.
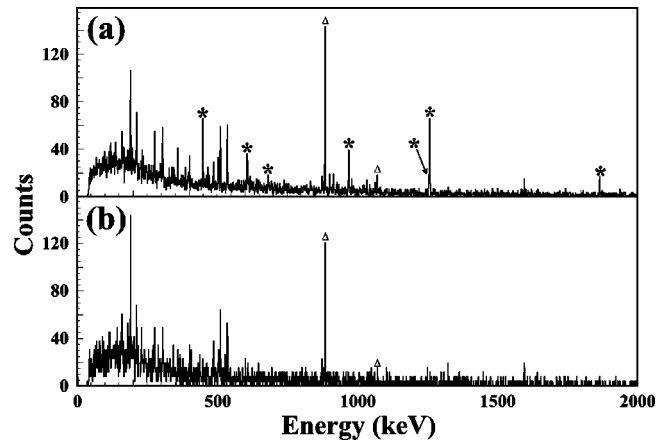

FIG. 8. Representative β-gated γ-ray spectra for $A=70$ when (a) lasers are tuned to Co resonance and (b) lasers are off. The asterisks indicate lines that can be positively associated with ^{70}Co decay and triangles indicate γ rays from the ^{70}Ni daughter decay.

The decay scheme for ^{70}Co is presented in Fig. 10. Based on the relative intensities of the γ rays in β-gated spectra, the β branching ratios and $\log ft$ values can be deduced. These are also presented in the figure. Due to the very large Q value (~ 12 MeV [27]) and from what is observed in ^{68}Co decay, it is very likely that there are weaker γ-ray branches that are not observed. As a consequence, all β branching ratios and $\log ft$ values presented in Fig. 10 are limits.

IV. INTERPRETATION OF THE DECAY SCHEMES

A. ^{66}Co

The ground state of ^{66}Co was tentatively assigned by Bosch *et al.* [20] to be the 3^+ member of the $\pi f_{7/2}^{-1} \nu p_{1/2}^{-1}$ configuration. The favored decay mode for such a configuration is a Gamow-Teller conversion of a $f_{5/2}$ neutron particle to fill the $f_{7/2}$ proton hole. Thus the most strongly fed levels in ^{66}Ni will have $\nu f_{5/2}^{-1} \nu p_{1/2}^{-1}$ as a significant part of their wave function. The strongest feeding is observed to a
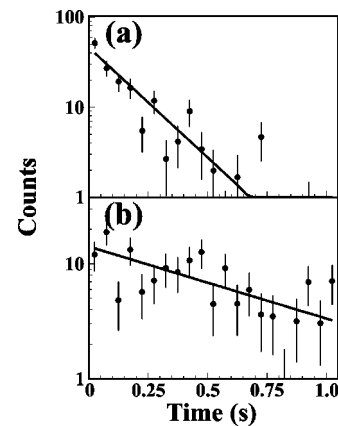

FIG. 9. Time dependent spectra for the 0.6/1.0 s macrocycle when (a) gated on long half-life γ rays of Table IV and (b) short half-life γ rays. The thick lines show the results of decay fits to the data.

TABLE IV. Energy, relative intensity, and half-life identification of γ rays measured in β-gated decay spectra of ^{70}Co. The left columns correspond to the γ rays with 0.12(3) s half-lives, and the right columns those with 0.50(18) s half-lives. The intensities are normalized with respect to the isomer from which they originate.

$t_{1/2}=0.12(3)$ s		$t_{1/2}=0.50(18)$ s	
Energy (keV)	Intensity (relative)	Energy (keV)	Intensity (relative)
448.9(2)	81(5)	607.6(2)	$\equiv 100(10)$
682.8(2)	53(5)	1256.8(2)	40(10)
969.9(2)	$\equiv 100(7)$	1259.6(2)	280(28)
1259.6(2)	102(10)	1867.7(2)	75(10)

level at 2672 keV; however, this level was tentatively assigned as 0^+ in Ref. [22]. Based on the strong feeding observed to this level ($\log ft = 4.2$), a more likely assignment is 3^+ with $\nu f_{5/2}^{-1} \nu p_{1/2}^{-1}$ as its primary configuration. A similar conclusion was made by Pawłat *et al.* [5]. A 2_2^+ level at 2900 keV more clearly assigned from Ref. [22] might have been the 2^+ partner of this configuration, however, this level is not observed in this study. Feeding with a $\log ft$ of 4.5(12) was observed to the 2_3^+ level at 3231 keV, which suggests that this is the 2^+ partner to the 3^+ state. The fact that feeding is observed to the 1426-keV level but no significant β branching is seen to the 2900-keV state, brings into doubt the 2^+ assignment of the 2900-keV level.

B. ^{68}Co

Probable configuration and spin assignments for the two isomeric states in ^{68}Co can be made by comparison with odd-A Co and Ni isotopes. With $Z=27$ the proton configuration observed in Co nuclei is $\pi f_{7/2}^{-1}$ with a consequent spin and parity for the ground states of odd-A Co nuclei of $7/2^-$.
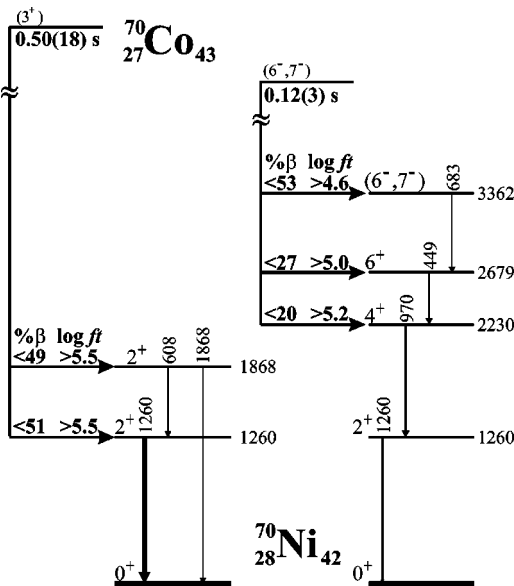

FIG. 10. The decay scheme for ^{70}Co. Decays of the two isomers are shown separately.

This can be seen, for example, in Refs. [11,12,20]. The neutron number for ^{68}Co is $N=41$ and neutron single-particle configurations can be deduced by comparison with levels in $^{69}_{28}$Ni$_{41}$. ^{69}Ni is observed to have two β decaying isomers with spins and parities of $9/2^+$ and $1/2^-$ [12]. The configuration of these two states have been interpreted as $\nu g_{9/2}^{+1}$ and $\nu p_{1/2}^{-1} \nu g_{9/2}^{+2}$, respectively. Thus the two isomers observed in ^{68}Co are formed by the coupling of an $f_{7/2}$ proton hole to the $\nu g_{9/2}^{+1}$ and $\nu p_{1/2}^{-1} \nu g_{9/2}^{+2}$ configurations. Based on studies for coupling the angular momentum of particle and hole states [28,29] the lowest state of the $\pi f_{7/2}^{-1} \nu g_{9/2}^{+1}$ multiplet is the $I_1 + I_2 - 1$ level, namely 7^- (denoted later as the high-spin state). Additional justification for this assignment, comes from comparison to the $\pi g_{9/2}^{-1} \nu g_{9/2}^{+1}$ states in ^{90}Nb [27] where the $I_1 + I_2 - 1$ level is indeed the lowest state of this multiplet. Using similar arguments, but for hole-hole coupling rather than particle-hole, the likely spin and parity of the $\pi f_{7/2}^{-1} \nu p_{1/2}^{-1} \nu g_{9/2}^{+2}$ configuration is 3^+ (referred to below as the low-spin isomer).

As stated in Sec. IV A, the most favored decay mode observed in Co nuclei is the Gamow-Teller $\nu f_{5/2} \rightarrow \pi f_{7/2}$ conversion and one would expect the same for ^{68}Co. Thus the decay of the high-spin state ($\pi f_{7/2}^{-1} \nu g_{9/2}^{+1}$) in ^{68}Co will proceed most strongly to states with a significant percentage of the $\nu f_{5/2}^{-1} \nu g_{9/2}^{+1}$ single-particle configuration in their wave function. What is observed in the decay of the short half-life state of ^{68}Co is strong feeding to two states at 3444 and 3558 keV with $\log ft$ values of 4.5(2) and 4.8(2), respectively, and a weaker fed level at 3120 keV with a $\log ft$ of 5.6(1). Based on the $\log ft$ values, it is likely that the 3444 and 3558 keV levels are the 7^- or 6^- states of the $\nu f_{5/2}^{-1} \nu g_{9/2}^{+1}$ multiplet. Thus, the high-spin value of 7^- is assigned to the short half-life β decaying state in ^{68}Co. If one considers a simple δ interaction, then the even spin states resulting from a $\nu f_{5/2}^{-1} \nu g_{9/2}^{+1}$ coupling would be unperturbed, while odd spin states would be increasingly lowered with the smallest odd spin being the most perturbed. Thus the 3558-keV level is most likely 6^- and the 3444-keV state 7^-. From energetic considerations the 3120-keV level could be the 5^- level of this multiplet; however, a $\log ft$ value of 5.6(1) is much too low for $7^- \rightarrow 5^-$ forbidden transition. Nevertheless, it is possible that this apparent intensity is the result of feeding from higher levels and consequently the $\log ft$ is smaller than the true value. Also note that these spin assignments are in disagreement with those reported in Ref. [26].

The $\nu f_{5/2} \rightarrow \pi f_{7/2}$ Gamow-Teller decay of the low-spin isomer ($\pi f_{7/2}^{-1} \nu p_{1/2}^{-1} \nu g_{9/2}^{+2}$) will most favorably populate levels with $\nu f_{5/2}^{-1} \nu p_{1/2}^{-1} \nu g_{9/2}^{+2}$ as part of their single-particle configuration. The expected energy for such a transition can be deduced from the comparison with the decay of ^{66}Co (see Sec. IV A). In ^{66}Ni, the $\nu f_{5/2}^{-1} \nu p_{1/2}^{-1}$ states are observed at energies of 2672 and 3228 keV. In ^{68}Ni there must also be an excitation of a pair of neutrons into the $g_{9/2}$ orbital, and as a consequence require an additional ~ 1.8 MeV of energy. Thus the expected energy of the ($\nu f_{5/2}^{-1} \nu p_{1/2}^{-1} \nu g_{9/2}^{+2}$) multiplet would be ~ 4.5 MeV, and it would be expected from the comparison with ^{66}Co decay that these levels in ^{68}Ni would

be fed from the decay of the low-spin isomer in ^{68}Co with log ft values of 4.1 to 5.0.

There are no strongly fed levels observed at $\sim$4.5 MeV; however, as noted in Sec. III B, $\approx$50% of the β feeding from the low-spin isomer may occur to unobserved levels, thus some of this intensity may be to several levels near that energy. It is also possible that the levels at 4027 and 4165 keV could be from the $\nu f_{5/2}^{-1} \nu p_{1/2}^{-1} \nu g_{9/2}^{+2}$ multiplet. The levels at $\sim$5.5 MeV, however, are unlikely to be this configuration since they are more than 1 MeV higher than the expectation. Nevertheless, it is clear that there exists a significant structure change when going from ^{66}Ni to ^{68}Ni. The results suggest that either there is no state with a dominant $\nu f_{5/2}^{-1} \nu p_{1/2}^{-1} \nu g_{9/2}^{+2}$ configuration in its wave function or that the configuration of the ^{68}Co isomer is strongly mixed.

In order for the 5^- level at 2848 keV in ^{68}Ni to be isomeric, states below this level are restricted in spin to $\leqslant$2. Thus possible spin assignments for the 2511 and 2745-keV states are restricted to 0^+ and 2^+.[1] An assignment of 2^+ can be made for the 2745-keV level because of an observed strong γ-ray branch to the ground state. A similar ground-state transition for the 2511-keV level is not observed. While a 2^+ assignment for this state cannot be ruled out, the lack of observed ground-state feeding provides support for a 0^+ assignment. With such an assignment, one can consider that the source of 511 keV γ-rays could be from the $E0$ decay of the 2511-keV level to the ground state. In this case, one would expect to observe the 1515-keV transition in coincidence with the 511-keV γ rays. It is estimated that four photopeak-photopeak events should have been observed if this was the case; however, no 1515-511 coincidences were recorded. Nevertheless, if these 511-keV γ rays indeed result from a 2511-keV $0_3^+ \rightarrow 0_1^+$ decay, one can estimate the strength parameter (ρ^2) of this transition. As noted in Sec. III B, the limit of the half-life for the 511-keV γ ray is $<$15 ns. Using a procedure similar to that presented in Ref. [25] for calculating ρ^2 of the 0_2^+ decay in ^{68}Ni, one can obtain a limit on ρ^2 for the $0_3^+ \rightarrow 0_1^+$ transition of $>$0.24 if all the intensity of 511-keV γ ray originates from this level.

The log ft values to the 3148, 3542, and 3987 keV levels are consistent with forbidden transitions. Ishii *et al.* [26] observed the 3148 keV level from the γ decay of the 8^+ isomer, thus fixing the spin of this level as 4^+. The other two levels (3542 and 3987 keV) are observed to γ decay directly to the 2848 keV state and are fed by β decay of the low-spin isomer. Since they are β fed from a 3^+ state and γ decay to a 5^- state, this restricts their spin assignments to 3^- or 4^-. The 3^- state in the $^{90}_{40}$Zr$_{50}$, the valence mirror to ^{68}Ni, is observed to feed the 2_1^+ level rather than the 5_1^- state. Since the 3542 and 3987-keV levels are not observed to feed the 2_1^+ state, it is likely that they are both 4^-, however 3^- cannot be ruled out. These two states could arise from the $\nu p_{1/2}^{-1} \nu g_{9/2}^{+1}$ and $\nu f_{5/2}^{-1} \nu g_{9/2}^{+1}$ configurations, and the similar

log ft values to these levels implies that these states are rather heavily mixed.

The lowest log ft values from the low-spin isomer decay is observed to states $>$5.5 MeV in excitation energy. At this energy it is possible to have proton excitations across the Z $=$28 gap. For example, proton particle-hole states probed by transfer reactions are observed at $\approx$4 MeV in ^{64}Ni [30]. These states could be populated in ^{68}Ni by $\nu p_{1/2} \rightarrow \pi p_{3/2}$ Gamow-Teller decay. Such a favored decay of the low-spin isomer must leave a $\nu g_{9/2}$ pair excitation across the N=40 gap since this is a component of the low-spin isomer wave function. Thus the levels most favorably fed will have a $\pi f_{7/2}^{-1} \pi p_{3/2}^{+1} \nu p_{1/2}^{-2} \nu g_{9/2}^{+2}$ configuration. The expected energy of such a configuration would be $\sim$6 MeV. What is observed experimentally is relatively strong feeding to levels at $\sim$5.5 MeV with log ft values of 5.7, 5.8, and 5.4. Thus, these levels at 5517, 5554, and 5778 keV are likely the 2^+, 3^+, and 4^+ members of the $\pi f_{7/2}^{-1} \pi p_{3/2}^{+1} \nu p_{1/2}^{-2} \nu g_{9/2}^{+2}$ single-particle configuration. While it was suggested earlier that the two levels at 4027 and 4165 keV could have $\nu f_{5/2}^{-1} \nu p_{1/2}^{-1} \nu g_{9/2}^{+2}$ as their primary configuration, it is also possible that the $\pi f_{7/2}^{-1} \pi p_{3/2}^{+1}$ configuration is a considerable part of the wave function. Since this latter configuration does not have a $g_{9/2}$ neutron pair component, one might expect very retarded β feeding to these levels; however, it was shown in Ref. [12] that there is strong mixing between $0p$-$0h$ and $2p$-$2h$ configurations around the N=40 gap, and thus the only slightly larger log ft values of 6.0 and 5.9 for the $\sim$4 MeV states compared to the $\sim$5.6 values for the $\sim$5.5 MeV states would be consistent with a large mixing.

C. ^{70}Co

The spin assignments for the states in ^{70}Co and ^{70}Ni can follow by analogy with ^{68}Co and ^{68}Ni. In this case, ^{70}Co has an additional two neutrons compared to ^{68}Co, and consequently the primary single-particle configurations of the high-spin and low-spin states are $\pi f_{7/2}^{-1} \nu g_{9/2}^{+3}$ and $\pi f_{7/2}^{-1} \nu p_{1/2}^{-1} \nu g_{9/2}^{+4}$, respectively. Thus, the likely spin and parity assignment for the short half-life state is 6^- or 7^-, and 3^+ for the long half-life isomer. It is interesting to note that even with the addition of a pair of $g_{9/2}$ neutrons the isomerism observed in ^{68}Co persists in ^{70}Co.

The level at 3361 keV in ^{70}Ni is fed by the high-spin state of ^{70}Co with a log ft value of $\approx$4.6. From the comparison with ^{68}Co, it is likely that this level at 3361 keV has I^π $=6^-$ or 7^- with a primarily $\pi f_{5/2}^{-1} \nu g_{9/2}^{+3}$ single-particle configuration. Unlike ^{68}Co, this level is not observed to decay to the 5^- level but rather to the 6^+ level at 2678 keV. The decay of the low-spin isomer in ^{70}Co is observed to proceed through the 1259 and 1867-keV levels. If this were direct feeding, then these levels would have log ft values of 5.5; however, from the comparison with ^{68}Co, it is likely that nearly all of the intensity comes from unresolved γ rays that decay from higher energy excited states. Nevertheless, since direct ground-state feeding is observed from the 1867-keV state the probable spin and parity of this level is 2^+.

---

[1]States with spin 1 cannot be formed at such a low energy and thus can be removed from consideration immediately.

V. COMMENT ON HALF-LIVES

The experimental half-lives have been compared with two quasiparticle random-phase appoximation (QRPA) calculations [31]. The first set of calculations used the Nilsson potential with BCS pairing (Nil-BCS) to calculate the single-particle energies, and the second set was performed for a folded-Yakawa potential with the Lipkin-Nogami pairing prescription (FY-LN). The calculated half-lives from these two sets are presented with the experimental data in Table II. In general, both calculations are very similar and predict on average half-lives that are about twice as fast as the experimentally observed values. The best agreement is observed in ^{66}Co where the calculated values of 0.137 s and 0.212 s for the Nil-BCS and FY-LN approaches, respectively, are in good agreement with the experimental value of 0.18(1).

Hannawald *et al.* [32] recently showed that a similar amount of deviation is also observed in the half-lives of $^{61-67}$Mn data. These differences in Mn as well as in Co are in contrast to the results of half-life calculations for neutron-rich Ni isotopes [10] where the agreement with experiment was quite good. The deviation observed in the Co decay half-lives is likely the result of deformation in the Co nuclei. The results from potential-energy surface calculations [33] indicate a rather complex mixture of prolate, oblate, and spherical shapes for the Co nuclei, while the Ni nuclei have a very deep spherical minimum. These differences in the energy surfaces are not included in the QRPA model and consequently the wave functions in Co nuclei are calculated to be more pure than what would be expected from a complex mixing of states.

VI. DISCUSSION

Ni isotopes have a closed proton shell; thus, it is neutron excitations within the fp shell and $g_{9/2}$ orbital that dominate the level structure of ^{58}Ni up to the heaviest isotope with known excited states ^{70}Ni. These nuclei can be compared with $N=50$ isotones from $Z=30$ to 42. In this case, the proton excitations in the fp and $g_{9/2}$ orbitals dictate the structure. Thus, these nuclei can be considered the valence mirrors of the Ni isotopes.

The similarity between these two groups can be seen in Fig. 11(a) where the 2_1^+ and 2_2^+ states of the even-even Ni and $N=50$ nuclei are plotted. It can be seen that for N and $Z \leqslant 38$ the similarity between excitation energies of these levels is remarkable. For N or $Z > 38$, one observes that the 2_1^+ states continue to have similar excitation energies; however, the 2_2^+ levels in ^{68}Ni$_{40}$ and ^{70}Ni$_{42}$ are progressively lower in energy compared to what is observed in $^{90}_{40}$Zr and $^{92}_{42}$Mo.

Negative parity 5_1^- and 7_1^- levels resulting from $p_{1/2}^{-1}g_{9/2}^{+1}$ and $f_{5/2}^{-1}g_{9/2}^{+1}$ configurations are plotted in Fig. 11(b). One can observe that these levels also agree very well between the Ni isotopes and $N=50$ isotones, with the exception of ^{90}Zr. While the ^{68}Ni levels closely agree with the systematic trends in the $N=50$ isotones, the 5_1^- state in ^{90}Zr is ~500 keV lower than the systematic trend would suggest. In addi-
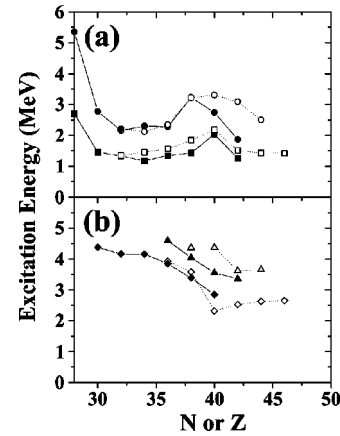

FIG. 11. Comparison of the excitation energy of (a) the 2_1^+ (squares) and 2_2^+ (circles) states, and (b) 5_1^- (diamonds) and 7_1^- (triangles) states. The filled symbols are even-even Ni isotopes plotted as a function of their neutron number and the open symbols $N=50$ isotones plotted against proton number.

tion, the 7_1^- state is an equivalent amount too high compared to the systematic trend.

It can be concluded that while there are many similarities observed in the comparison of Ni isotopes and $N=50$ isotones, there is a clear difference in the excitation of the 2_2^+ state. The negative parity states are also very similar with the exception of the apparently anomalous shifts observed in ^{90}Zr. In addition, the 0_3^+ state identified in ^{90}Zr is observed at 4126(3) keV, which is significantly higher than the 2511-keV level observed in ^{68}Ni.

Sinatkas *et al.* [34] successfully developed an interaction that incorporated the proton fp shell and $g_{9/2}$ orbital to interpret the nuclei at and below the $N=50$ gap. This interaction was also applied successfully in the interpretation of $A=64-67$ and 69 Ni isotopes [5,9,12]. These shell model calculations have now been extended to include ^{68}Ni and ^{70}Ni.

The results of the shell model calculations for ^{68}Ni and ^{70}Ni are compared with experiment and presented in Figs. 12 and 13. In these figures all the calculated and experimentally observed levels below 4.3 MeV and 3.6 MeV for ^{68}Ni and ^{70}Ni, respectively, are presented. For clarity the positive and
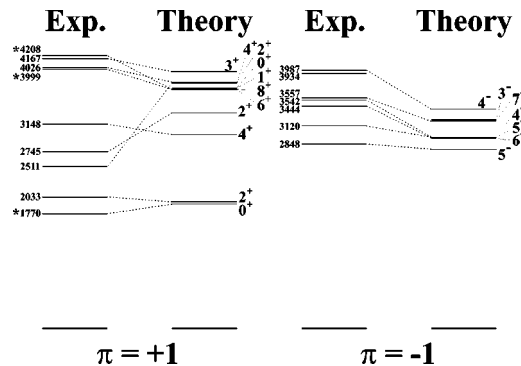

FIG. 12. Experimental and shell-model level schemes for ^{68}Ni. Experimental levels labeled with asterisks are levels observed by Bernas *et al.* [1] (1770) and Ishii *et al.* [26] (3999, 4208), but not observed in β decay.
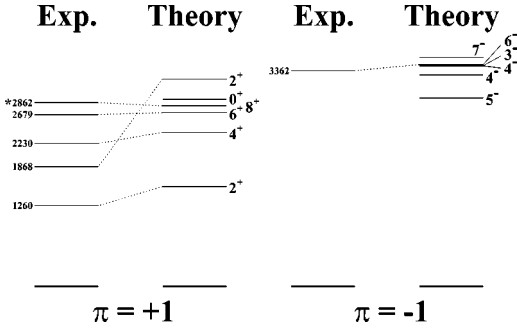
FIG. 13. Experimental and shell-model level schemes for ^{70}Ni. The experimental level labeled with an asterisk was observed by Grzywacz *et al.* [9] but not in β decay.

negative parity levels are separated in each case.

One can see from these results that good agreement is achieved for most of the levels. For example, the excitation energy for many of the positive parity states are well reproduced in both ^{68}Ni and ^{70}Ni. Good agreement is also achieved for the energy of the 5_1^- state in ^{68}Ni and the 7_1^- state in ^{70}Ni. The level ordering of the additional negative parity states (resulting from the $\nu p_{1/2}^{-1} \nu g_{9/2}^{+1}$ and $\nu f_{5/2}^{-1} \nu g_{9/2}^{+1}$ configurations) are reasonably well reproduced; however, the excitation energy of these levels tends to be predicted ~ 300 to 500 keV too low. Nevertheless, this agreement is very good. The levels most poorly reproduced are the 2_2^+ states in both ^{68}Ni and ^{70}Ni as well as the 0_3^+ state in ^{68}Ni. For ^{68}Ni the shell-model results are 583 keV higher than experiment, while for ^{70}Ni a 1362-keV difference exists. The results of the calculation place the 0_3^+ state at 3.7 MeV in ^{68}Ni, which is also significantly higher than what is observed. Since these differences were already observed from the comparison of the experimental levels of the valence mirror nuclei and the effective interaction was developed for the $26 < Z < 50$ region, it is perhaps not surprising that this difference also exists in the theoretical calculations. The results of the calculation, however, clearly show the difference between Ni isotopes and their valence mirrors at $N = 50$.

While this particular shell-model calculation poorly reproduces the 2511 and 2745-keV levels in ^{68}Ni, it should be noted that Hartree-Fock-Bogoliubov calculations predict the 0_3^+ and 2_2^+ states to occur at ≈ 2.3 and 2.4 MeV, respectively [25]. While the detailed structure of these states was not discussed, they clearly originate from collective excitations. Since this discrepancy between the experimental and theoretical energy of the 2_2^+ states does not occur until the $g_{9/2}$ orbital starts becoming significantly occupied, one can speculate that the $\nu g_{9/2}$ orbital has a larger influence on the collectivity of Ni isotopes than the $\pi g_{9/2}$ orbital has on $N = 50$ isotones. This may also be a consequence of the relative strengths of $Z = 28$ and $N = 50$ shell gaps. This speculation is further reinforced by the nonobservation of an 8^+ isomer with a half-life from 25 ns to 2 ms in ^{72}Ni [35], which is predicted by shell-model calculations. Thus theories developed for the neutron-rich Ni region that do not properly account for collective excitations may have serious short comings.

VII. SUMMARY

The β-delayed γ decay of ^{68}Co and ^{70}Co is studied for the first time, and the results are compared with new measurements of the β decay of ^{66}Co. The yields of these nuclei from the laser ion source are deduced and compared with other Co and Ni nuclei produced with the same source. These experimental yields are compared with theoretical fission cross sections, and it can be seen that while the form of the yield trend is well reproduced by the theoretical calculations, the cross sections are predicted to maximize about one mass unit farther from stability than what is observed. This corresponds to an approximately one order of magnitude over prediction for the production of Ni and Co nuclei far from stability. Nevertheless, with the recent improvements to the laser ion source (as discussed in Sec. II), it should be possible to study Ni and Co nuclei even farther from stability.

From the analysis of the β-delayed γ rays, there is a clear identification of the two β-decaying states in both ^{68}Co and ^{70}Co. The ground states of these two nuclei are likely $\pi f_{7/2}^{-1} \nu g_{9/2}^{+1}$ and $\pi f_{7/2}^{-1} \nu g_{9/2}^{+3}$, respectively, which couple to form states of 6^- or 7^-; isomers are formed by the excitation of a pair of neutrons into the $g_{9/2}$ orbital (i.e., $\pi f_{7/2}^{-1} \nu p_{1/2}^{-1} \nu g_{9/2}^{+2}$ and $\pi f_{7/2}^{-1} \nu p_{1/2}^{-1} \nu g_{9/2}^{+4}$) and the resulting odd neutron hole couples with of proton hole to form 3^+ states.

The decay of the high-spin state in ^{68}Co is observed to feed most strongly states that can be identified as originating primarily from $\nu f_{5/2}^{-1} \nu g_{9/2}^{+1}$ broken pair configurations. A similar observation is made in the decay of ^{70}Co. These newly identified negative parity states in ^{68}Ni and ^{70}Ni compared with similar levels in lighter Ni isotopes are observed to be systematically lowered in energy with increasing neutron number. This is consistent with what is observed in $N = 50$ isotones with $30 < Z < 46$ which can be considered as the valence mirrors of the Ni isotopes.

Significant changes are observed in the decay of the 3^+ states when going from ^{66}Co to ^{68}Co and ^{70}Co. The β decay of ^{66}Co is observed to have a half-life of 0.18(1) s and proceeds to levels that can be identified as the two members of the $\nu f_{5/2}^{-1} \nu p_{1/2}^{-1}$ multiplet in ^{66}Ni. In ^{68}Ni, similar levels are expected to be ≈ 1.8 MeV higher in excitation energy due to the requirement to excite a pair of neutrons into the $g_{9/2}$ orbital; however, β decay to such levels could not be clearly identified. The decay of the 3^+ isomer in ^{68}Co is also clearly different from ^{66}Co in the fact the half-life is measured to be 1.6(3) s. Such a long half-life indicates that the wave function of the 3^+ state in ^{68}Co is strongly mixed or that there is no state in ^{68}Ni that has a dominant $\nu f_{5/2}^{-1} \nu p_{1/2}^{-1} \nu g_{9/2}^{+2}$ component. Because of this, other decay modes such as the $\pi p_{3/2} \rightarrow \nu p_{1/2}$ Gamow-Teller decay and forbidden decay to negative parity states compete with the $\nu f_{5/2} \rightarrow \nu f_{7/2}$ decay which is dominant in ^{66}Co. The half-life of the decay of the 3^+ state in ^{70}Co is shorter than what is observed in ^{68}Co, but is still long enough that one can make similar arguments for this nucleus.

The excited states observed in the ^{68}Ni and ^{70}Ni are compared with shell-model calculations as well as with their valence mirror $N = 50$ isotones. In general, the agreement is

quite good; however, a key feature that is very poorly reproduced is the location of the 2_2^+ states in both ^{68}Ni and ^{70}Ni. In addition, there is experimental evidence for a 0_3^+ state at 2511 keV in ^{68}Ni, but the 0_3^+ state from the shell model is at 3.7 MeV. The excitation energy of the 0_3^+ and 2_2^+ levels in ^{68}Ni are reasonably well reproduced by Hartree-Fock-Bogoliubov calculations, and from this comparison one can conclude that the lowering of these levels is likely due to significant influence from collective excitations. Similar excitations are not evident in the $N=50$ isotones, which is an indication of the difference between the $Z=28$ and $N=50$ shell gaps. Thus to describe ^{68}Ni and ^{70}Ni and possibly even heavier nuclei, collective excitations in addition to single-particle excitations should be considered.

[1] M. Bernas *et al.*, J. Phys. (France) Lett. **45**, L851 (1984).
[2] M. Bernas *et al.*, Phys. Rev. Lett. **67**, 3661 (1991).
[3] H. L. Seifert *et al.*, Z. Phys. A **349**, 25 (1994).
[4] Ch. Engelmann *et al.*, Z. Phys. A **352**, 351 (1995).
[5] T. Pawłat *et al.*, Nucl. Phys. **A574**, 623 (1994).
[6] R. Broda *et al.*, Phys. Rev. Lett. **74**, 868 (1995).
[7] F. Ameil *et al.*, Eur. Phys. J. A **1**, 275 (1998).
[8] O. Sorlin *et al.*, Nucl. Phys. **A660**, 3 (1999).
[9] R. Grzywacz *et al.*, Phys. Rev. Lett. **81**, 766 (1998).
[10] S. Franchoo *et al.*, Phys. Rev. Lett. **81**, 3100 (1998).
[11] L. Weissman *et al.*, Phys. Rev. C **59**, 2004 (1999).
[12] W. F. Mueller *et al.*, Phys. Rev. Lett. **83**, 3613 (1999).
[13] K.-L. Kratz *et al.*, Z. Phys. A **332**, 419 (1989).
[14] Y. Kudryavtsev *et al.*, Nucl. Instrum. Methods Phys. Res. B **114**, 350 (1996).
[15] L. Vermeeren *et al.*, Nucl. Instrum. Methods Phys. Res. B **126**, 81 (1997).
[16] P. Van den Bergh *et al.*, Nucl. Instrum. Methods Phys. Res. B **126**, 194 (1997).
[17] L. Weissman *et al.*, Nucl. Instrum. Methods Phys. Res. A **423**, 328 (1999).
[18] Y. Kudryavtsev *et al.* (unpublished).
[19] M. Huhta *et al.*, Phys. Lett. B **405**, 230 (1997).
[20] U. Bosch *et al.*, Nucl. Phys. **A477**, 89 (1988).
[21] S. Czajkawski *et al.*, Z. Phys. A **348**, 267 (1994).
[22] W. Darcey *et al.*, Nucl. Phys. **A170**, 253 (1971).
[23] U. Fister *et al.*, Phys. Rev. C **42**, 2375 (1990).
[24] N. B. Gove and M. J. Martin, Nucl. Data, Sect. A **10**, 205 (1971).
[25] M. Girod *et al.*, Phys. Rev. C **37**, 2600 (1988).
[26] T. Ishii *et al.*, Phys. Rev. Lett. **84**, 39 (2000).
[27] R. B. Firestone, *Table of Isotopes*, edited by V. S. Shirley (Wiley, New York, 1996), Vol. I.
[28] M. Moinester *et al.*, Phys. Rev. **179**, 984 (1969).
[29] V. Paar, Nucl. Phys. **A331**, 16 (1979).
[30] B. Singh, Nucl. Data Sheets **62**, 614 (1991).
[31] P. Möller and J. Randrup, Nucl. Phys. **A514**, 1 (1990).
[32] M. Hannawald *et al.*, Phys. Rev. Lett. **82**, 1391 (1999).
[33] P. Möller (private communication).
[34] J. Sinatkas *et al.*, J. Phys. G **18**, 1377 (1992); **18**, 1401 (1992).
[35] R. Grzywacz *et al.* (private communication).